J Biosci (2019) 44:142
DOI: 10.1007/s12038-019-9960-9

Iris yellow spot virus–induced chloroplast malformation results in male sterility

Ahmed Abdelkhalek[1], Sameer H Qari[2]* and Elsayed Hafez[1]

[1]*Plant Protection and Biomolecular Diagnosis Department, ALCRI, City of Scientific Research and Technological Applications, New Borg El Arab City, Alexandria, Egypt*

[2]*Biology Department, Al-Jumum University College, Umm Al-Qura University, Mecca, Saudi Arabia*

**Corresponding author (Email, shqari@uqu.edu.sa)*

MS received 27 April 2019; accepted 31 August 2019; published online 25 October 2019

Iris yellow spot virus (IYSV) is one of the most devastating viral pathogens, which causes high economic losses in the onion yield. Physiological and genetic changes are associated with the appearance of chlorotic symptom in the infected plants. IYSV-N gene sequence analysis revealed that it shared sequence identity of 99% with other Egyptian isolates, at both genomic and proteomic levels. In addition, N protein sequence with computational examination indicated many motifs involved and played different roles in the virus activity and its regulation and stability were detected. In the Differential Display-Polymerase Chain Reaction (DD-PCR) study, a highly up-regulated gene at 15 days post-biological IYSV inoculation (dpi) was selected for sequencing. Based on the sequencing results that showed the identified gene was coding for a chloroplast-related gene, degenerate specific primers were designed for Real-Time PCR analysis. A significant change in the transcription level of the chloroplast-related gene after 15 dpi suggested that some IYSV proteins interact and/or regulate with chloroplast proteins and this finding supports the DD-PCR results. At 20 dpi, the ultrathin sections showed that IYSV infection caused many dramatic chloroplasts malformations. The malformation appeared as chloroplast broken envelope with the presence of numerous spherical particles inside it and chloroplasts with long stromule. Our findings indicated that IYSV interrupts normal chloroplast functions, as a part of the onion defence response, however many crucial factors remain to be elucidated and further studies are needed at both biological and molecular levels.

Keywords. Chloroplast; defence system; electron microscope; *Iris yellow spot virus*; onion

1. Introduction

Onion (*Allium cepa* L.) is an economically important plant, cultivated worldwide. According to FAOSTAT data, Egypt is the fifth largest exporter of onion in the world after China, India, USA and Iran. Egypt currently produces approximately 2379035 tonnes from 68053 hectares and its production is increasing every year (FAOSTAT, 2017). *Iris yellow spot virus* (IYSV), genus *Tospovirus*, family *Bunyaviridae,* is one of the critical viral pathogens that causes disastrous losses by reduction of, both, the yield and/or quality of onion crop worldwide (ElMorsi *et al.* 2015; Abdelkhalek *et al.* 2018). Due to its transmission through thrips (*Thrips tabaci* L.), there has been high spread of this virus in many onion-growing countries all over the world (Fauquet *et al.* 2005; Hafez *et al.* 2012).

Usually, viral infection appears as symptoms resulting in morphological and physiological changes in the infected hosts (Zhao *et al.* 2016). The most common IYSV symptoms are spindle-shaped, straw-coloured, irregular, eye-like, or diamond-shaped, lesions and chlorotic changes reflecting the altered structure of leaf chloroplasts (Gent *et al.* 2006). The disorders in chloroplast components and their functions are liable for the production of chlorosis and yellowing symptoms that are associated with plant viral infection (Zhao *et al.* 2016).

Chloroplasts play important roles in plant defence against all the types of stresses (Serrano *et al.* 2016), thus some plant pathogens can affect some functions served by chloroplasts, i.e., photosynthesis (de Torres Zabala *et al.* 2015). Viruses mostly target the chloroplasts, causing huge structural and functional changes in the infected cells (Caplan *et al.* 2008; Bhattacharyya and Chakraborty 2018). A large number of plant viruses are capable of inducing the plant cells to produce virus-like particles (inclusion bodies) as a a plant-immune response against the virus attack (Edwardson *et al.* 1993). Many chloroplast-related proteins localised in the chloroplast or functionally related to the photosynthetic machinery, supporting viral propagation, as well as antiviral defence, may be induced upon viral infection (Qiao *et al.* 2009; Seo *et al.* 2014).

It is well known that invading pathogens activate the plant immune system and, in many cases, this enables the

development of resistance (Hafez *et al.* 2013). It has been reported that plants have their own immune mechanism by which they resist the pathogen attack after recognising it (Karimi *et al.* 2013). Besides its role in providing beneficial information on the morphology of the virus particles, Transmission Electron Microscopy (TEM) is also used to study the different cytopathological effects in infected plant cells (Otulak *et al.* 2014).

Usually, viral infections cause a fluctuation in the gene expression of some defence genes in the infected plant (Whitham *et al.* 2006). Differential Display-Polymerase Chain Reaction (DD-PCR) could be a powerful technique for the rapid identification of differentially expressed genes (Liang and Pardee 1992; Abdelkhalek *et al.* 2018). In addition, Real-time quantitative PCR (qRT-PCR) is a very accurate, reliable, and sensitive technique capable of detecting low amounts of RNA molecules in the tested sample; therefore, it can be considered as an efficient tool for quantifying the gene expression in any biological sample (Li *et al.* 2012). In this study, we highlight the effect of the IYSV infection on the plant cell level and how this effect could be prolonged to control developmental and functional processes. We then describe the virus-developed structural and functional damage of the chloroplasts presented in the infected plant cell, either by using Electron Microscopy and/or by molecular techniques. In addition, we speculate how the plant triggers an immune response via the interaction between the chloroplast and the pathogenic virus. Overall, we hypothesise how IYSV may not affect some chloroplasts genes but how it can also reach the mitochondrial genes and finally result in male sterility.

2. Materials and methods

2.1 *Virus isolate*

Onion leaf samples exhibiting characteristic IYSV-like symptoms were collected from the open fields at Alexandria government in Egypt. By using double antibody-sandwich enzyme-linked immunosorbent assay (DAS-ELISA), the collected samples tested for viral infection, as described previously by Clark and Adams (1977). The virus isolate was maintained continuously on *Datura stramonium* plants by mechanical inoculations in an insect proof greenhouse.

2.2 *Molecular detection of IYSV*

Total RNA from infected, as well as healthy, onion tissues was extracted using RNeasy Mini Kit (QIAGEN, Germany) according to the manufacturer's instructions. One microgram of RNA was utilised in order to synthesise cDNA using oligo (dT) primer with Superscript reverse transcriptase enzyme according to the manufacturer's instructions (Invitrogen, USA). 1 µl of cDNA was used for PCR amplification of the IYSV nucleocapsid protein using specific primers (table 1). The PCR amplification product was purified by a PCR clean-up column kit (QIAGEN, Germany) and checked on agarose gel electrophoresis. After the sequencing process, the annotated nucleotide sequence was deposited in GenBank and compared with those of previously reported IYSV isolates.

2.3 *Thrips transmission and differential display-PCR analysis*

Biological transmission using thrips, *Thrips tabaci* Lindman, on healthy onion seedlings was performed according to Murai and Loomans (2001). Three biological replicates of viruliferous thrips transmission were collected at 5, 10, 15 and 20 days post inoculation (dpi). Mock-treated samples with non-viruliferous thrips were used as a control.

Total RNA extracts from all treatments were subjected to cDNA synthesis, using oligo (dT) with random hexamer primers (Hafez *et al.* 2013). The arbitrary prime RAPD10 (table 1) was used to scan the mRNA genes in infected plants, at intervals, and in healthy plants as well. The amplified cDNA was used as a template for the differential display (DD-PCR) reaction that was performed according to Abdelkhalek *et al.* (2018). Amplification products were visualised using a gel documentation system (Syngene, USA) in 1.5% agarose gel that was electrophoresed in 0.5X TBE buffer. The selected PCR band was excised from the gel, purified using a QIA quick gel extraction kit (Qiagen Inc., Germany) and sequenced. The obtained DNA nucleotide sequences were analysed using NCBI-BLAST (*http://blast.ncbi.nlm.nih.gov/Blast.cgi*) before deposited in GenBank.

Table 1. List of primers sequences used in this study

Primer	Direction	Sequence	Amplicon size	Reference
IYSV-N gene	Forward	TAAAACAAACATTCAAACAA	1100 bp	Pappu *et al*. (2006)
	Reverse	CTCTTAAACACATTTAACAAGCA		
RAPD10		ATGCCCCTGT		Hafez *et al*. (2013)
Chloroplast gene	Forward	GCACGACGCTTGTATTGCTC	158 bp	This study
	Reverse	TGAATCCATGGGCAGGCAAG		

2.4 *Primer design and quantitative PCR analysis*

Based on the chloroplast sequence obtained from the DD-PCR reaction (Ac# MH746819), two degenerate primers (table 1) were designed by the NCBI Primer blast software (*http://www.ncbi.nlm.nih.gov/tools/primer-blast/*) to amplify 158 bp within the chloroplast gene and used it as qRT-PCR specific primers. The primers sequence was checked by NCBI-BLAST online software. By using the SYBR Green PCR Master Mix (Fermentas, USA), qRT-PCR was performed according to the previous study (ElMorsi *et al.* 2015). The housekeeping gene β-actin was used as a reference gene and data were analysed according to Livak and Schmittgen (2001).

2.5 *Statistical analysis*

The relative expression values of three replicates for each set levels were analysed by one-way analysis of variance (ANOVA) with $P \leq 0.05$, using the CoStat software. The significant differences of the relative expression levels were plotted, and standard deviation (± SD) is shown as a column bar (figure 6). Relative expression levels more than 1 demonstrate an increase in accumulation (up-regulation) and values lower than 1 means a decrease in expression (down-regulation).

2.6 *Transmission electron microscopy examination*

Small sections from symptomatic onion leaves at 20 dpi were excised, fixed in 2.5 % glutaraldehyde buffered with 75 mM/L potassium phosphate, pH 7.0, for 2 h, and then prepared for TEM examination using standard procedures described by Martelli and Russo (1984) and Hafez *et al.* (2011). The ultrathin sections were examined with TEM, JEOL-CX100 operating at 80 KV (The electron microscope unit, Faculty of Science, Alexandria University, Egypt).

3. Results

3.1 *Detection and molecular characterisation of the IYSV-nucleocapsid (N) gene*

The characteristic symptoms of IYSV in samples showing positive infection judged by DAS-ELISA were recorded as eye-like or diamond-shaped lesions, necrotic, and chlorotic lesions on plant leaves. By using RT-PCR with specific IYSV-N gene primers, a molecular size band of 1100 bp was detected in the infected tissues only.

After PCR product purification, sequencing, and BLAST alignment, the annotated sequence submitted to GenBank database under the accession number KC122192. Results of the sequence analysis revealed that the N gene sequence contains a single open reading frame (ORF) of 822 nucleotides encoding for a protein of 273 amino acids (figure 1). The ATG codon for methionine amino acid, the start codon, was at the position 1 nucleotide, whereas the stop codon, TAG, was at the position of 820 nucleotides (figure 1). Out of the 273 amino acids, 41 strongly acidic amino acids and 33 strongly basic amino acids were detected in the deduced N gene polypeptide. The theoretical PIs was 9.09 and the full length was classified as stable [Instability Index (II): 30.46]. NCBI-BLAST and phylogenetic analysis indicated that the IYSV-Egyptian isolate is closely related to the other Egyptian isolates especially with the HafKal isolate (Acc# JN541273) with a 99% identity (figure 2).

Bioinformatics is an essential tool for analysing and identifying several motifs within the plant viruses' proteins sequence. The four motifs (figure 1) predicted for Protein kinase C phosphorylation site (3 aa; 10 sites), Casein kinase II phosphorylation site (4 aa; 6 sites), N-myristoylation sites (6 aa; 3 sites) and cAMP- and cGMP-dependent protein kinase phosphorylation site (4 aa; 1 site) were detected within the N gene (figure 1).

3.2 *Biological transmission and DD-PCR analysis*

The onion plants inoculated by viruliferous thrips showed symptoms identical to those reported on naturally IYSV-infected plants (data not shown). Comparing to mocked tissues at 5, 10, 15, and 20 dpi, all the inoculated plant tissues with viruliferous thrips gave positive results in PCR with IYSV-N gene specific primer (figure 3). In order to shine light on the molecular basis of the interaction between onion plants and IYSV, DD-PCR technique using RAPD10 primer was performed. The results revealed that RAPD10 primer succeeds to give about 62 different band patterns with molecular weights ranging from 180 bp to 1000 bp (figure 4). The highly polymorphic expressed band at 15 dpi with molecular size about 480 bp was selected, purified and sequenced. The sequence analysis revealed that the up-regulated gene encodes a chloroplast-related protein and it was deposited in GenBank database under the accession number MH746819. The sequence contains a single ORF of 440 nucleotides encoding a protein of 146 amino acids. Theoretically, the PI was 9.22. The gene peptide molecular mass calculated to be 16.05 kDa and the instability index (II) was computed to be 49.15. On the other hand, the NCBI-BLAST and phylogenetic analysis showed that the chloroplast gene is strongly associated to the other *Allium* chloroplast isolates especially with *Allium cepa* genotype normal (N) male fertile chloroplast (Acc# KF728079) with a 99% identity (figure 5).

3.3 *Expression of the chloroplast-related gene using qRT-PCR*

A specific degenerated primer amplifying 158 bp was designed to detect the level of chloroplast-related protein transcripts in

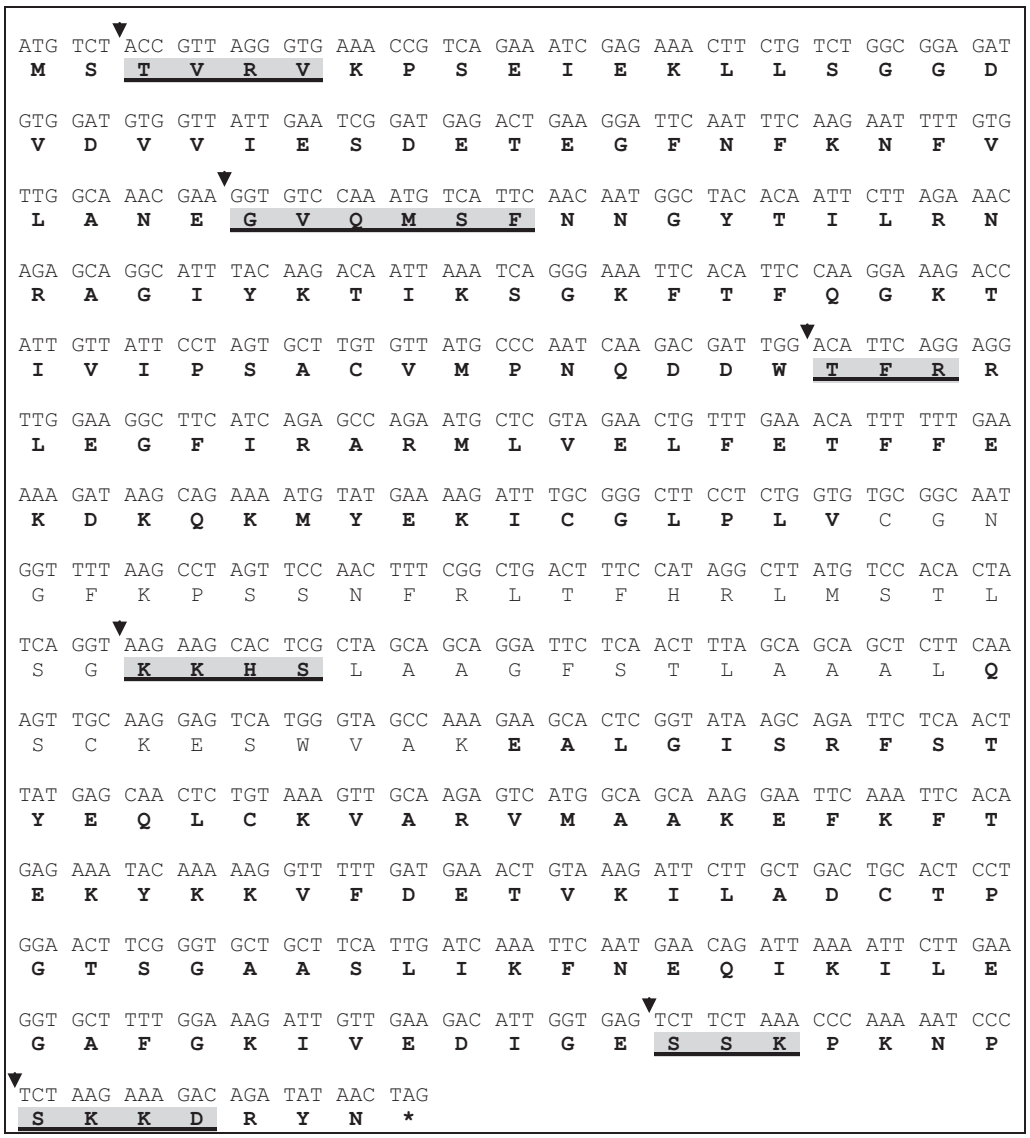

Figure 1. The complete nucleotide sequence of the nucleocapsid (N) gene of IYSV-Egypt (#KC122192) amplified from onion. The deduced amino acid sequence of the protein encoded by the viral sense RNA is shown below the DNA sequence. Potential Protein kinase C phosphorylation site (3 aa; 10 sites), Casein kinase II phosphorylation site (4 aa; 6 sites), N-myristoylation sites (6 aa; 3 sites) and cAMP- and cGMP-dependent protein kinase phosphorylation site (4 aa; 1 site) are underlined. Asterisks indicate the stop codons.

onion plants upon IYSV infection. The qRT-PCR results reflect the mathematical transformation of the *Ct* values of the examined gene and the relative expression analysis was normalised to the β-actin gene as an internal control for quantitative gene expression at 5, 10, 15 and 20 dpi as well as the mocked plant (control).

In comparing to mocked samples, the results revealed that the chloroplast-related protein is slightly down-regulated after 5 dpi with expression level 0.91-fold of the control (figure 6). The expression level was dramatically decreased to 0.054-fold compared with the control, at 10 dpi. At 15 dpi, the expression level up-regulated and increased rapidly with 2.46-fold of control (figure 6). Like 10 dpi, the expression level was down-regulated again at 20 dpi with 0.035-fold of the mocked. According to the one-way ANOVA analysis, the expression levels had significant differences at different time intervals (figure 6). Among these intervals, the expression at 15 dpi was up-regulated, and at 10 and 20 dpi, the level of expression was down-regulated. At 5 dpi, the expression showed a slight down-regulation and there was no statistically significant difference between the infected and mocked plants at this interval (figure 6).

3.4 *Transmission electron microscopy and cytopathological effects of IYSV*

When compared to ultrathin sections of mocked onion leaves that showed normal cell structure with normal chloroplast (data not showed), the infected leaves revealed

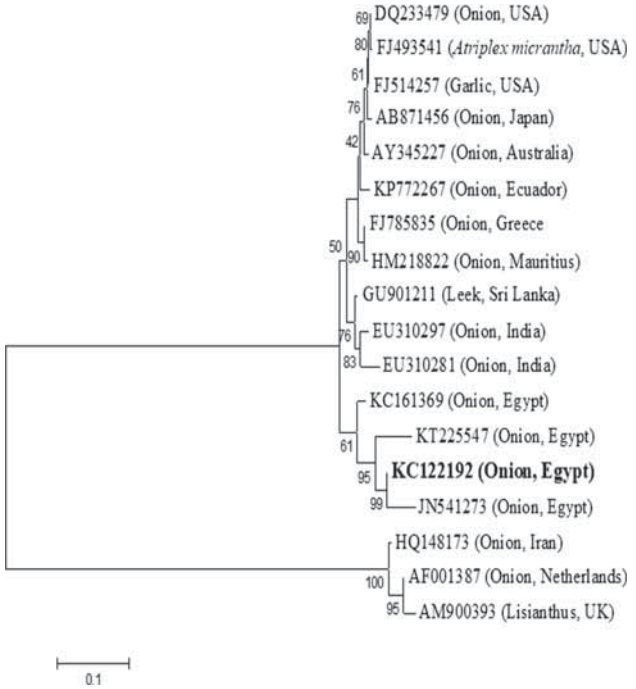

Figure 2. Phylogenetic analysis showing the genetic relationship between nucleotide sequence of the IYSV-N gene (KC122192) and other nucleocapsid genes available in GenBank. The phylogeny tested with bootstrap method with 2,000 replications and generated based on UPGMA statistical method.

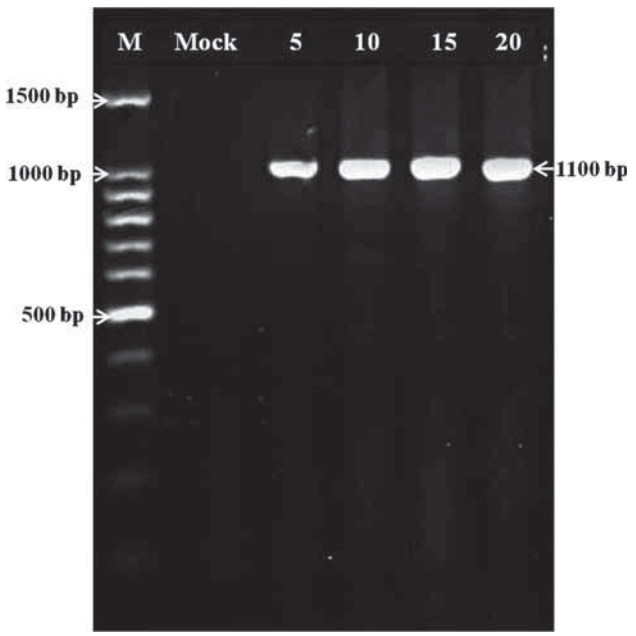

Figure 3. Agarose gel electrophoresis (1.5%) in TBE buffer stained with ethidium bromide, showing RT-PCR detection of IYSV-N gene in the infected onion at different time intervals compared to mocked plants. Lane M: 100bp Ladder DNA Marker; Lane Mocked: onion tissues inoculated with non-viruliferous thrips; Lanes 5,10,15 and 20: onion tissues collected at 5, 10, 15 and 20-day post inoculation with IYSV.

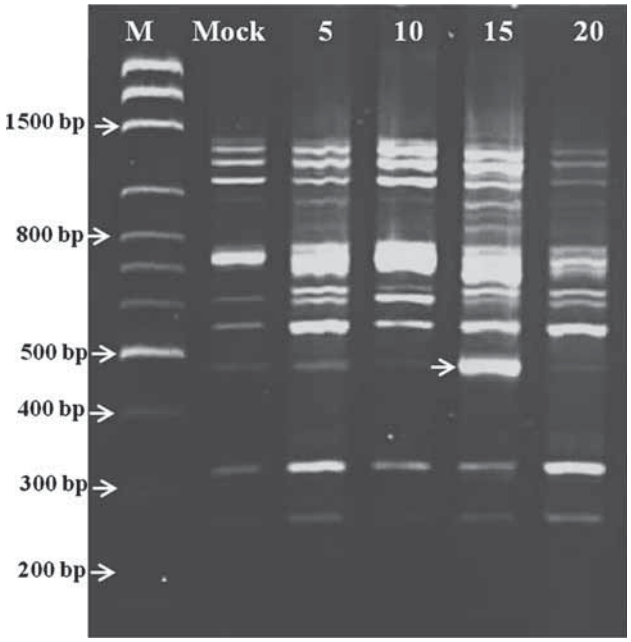

Figure 4. Agarose gel electrophoresis (1.5%) in TBE buffer stained with ethidium bromide, showing DD- PCR using primers RAPD 10. Lane Marker: DNA marker 100 bp ladder, lane 'Mock' control (mock-inoculated plant tissues), lanes 5, 10, 15 and 20: plant tissues collected at 5, 10, 15 and 20 dpi of viruliferous thrips inoculation. Black arrow indicates the bands that were selected for sequencing.

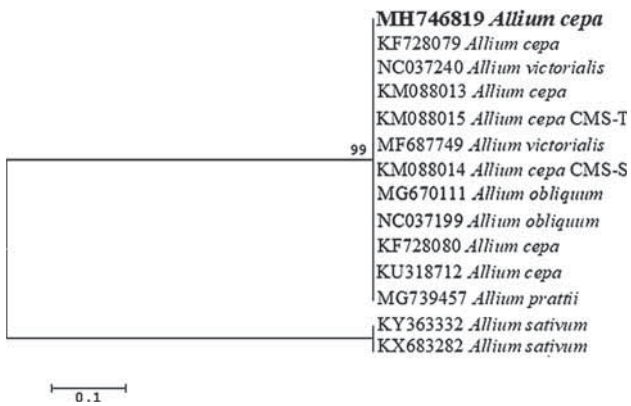

Figure 5. Phylogenetic analysis showing the genetic relationship between nucleotide sequence of the chloroplast-related gene (MH746819) and other related genes available in GenBank. The phylogeny tested with bootstrap method with 2,000 replications and generated based on UPGMA statistical method.

many cytopathological effects in the chloroplast organelles at 20 dpi (figure 7). The chloroplast malformations showed irregular outer-membrane structures and broken envelope with the presence of numerous spherical particles inside it (figure 7a). Moreover, chloroplast with long stromule was clearly detected (figure 7b). The more IYSV-like particles accumulated in chloroplast with more chloroplast aggregation (figure 7c). Partially destroyed and deformed

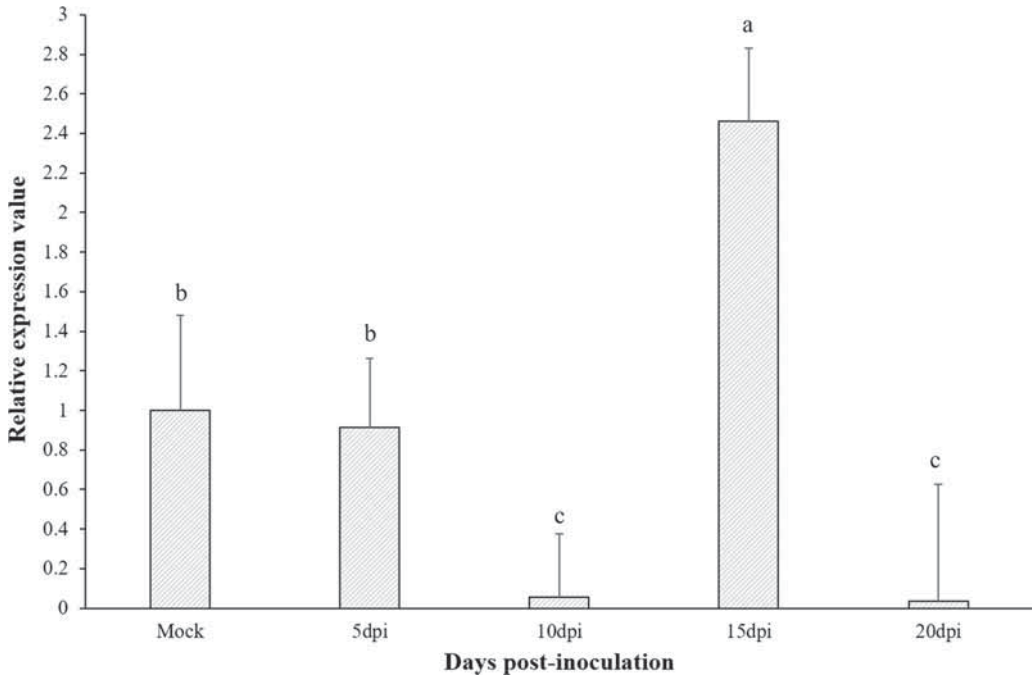

Figure 6. The relative expression levels of chloroplast-related gene upon IYSV infection at 5, 10, 15, and 20 dpi compared to mocked onion tissues. Columns represent mean value from three biological replicates and bars indicate Standard Deviation (±SD). Significant differences between samples were determined by one-way ANOVA using CoStat software. Means were separated by Least Significant Difference (LSD) test at $P \leq 0.05$ levels and indicated by small letters. Columns with the same letter means do not differ significantly.

chloroplasts with disorganised grana and stroma lamella were also detected (figure 7d).

4. Discussion

Onion is one amongst the foremost vital field crops grown in many Egyptian provinces, for both local consumption and exportation (Abdelkhalek *et al.* 2018). It is the third most valuable vegetable crop in Egypt and the second most valuable vegetables in the world (Vajire *et al.* 2017), so it is an essential crop in many parts of the world for subsistence and food security. Almost 66% of all onion is produced in Asia, followed by Africa, by 12.4% (FAOSTAT 2017). IYSV is one of the most damaging viral threats to onion crops all over the world, causing devastating losses of onion crop (Elmorsi *et al.* 2015).

The nucleocapsid (N) gene is the most common gene used for identification of tospoviruses. Thus, nucleotide sequence comparisons could be a useful method for viral classification and identification (Pappu *et al.* 2006). Until now, there is not enough data available on the nucleotide sequence of the Egyptian IYSV isolates. By using RT-PCR with specific IYSV-N gene primers, a band with a molecular size of 1100 bp was detected in the infected tissues only.

The N gene of Egyptian IYSV (Acc# KC122192) was 822 nucleotides long and could potentially code for a protein of 273 amino acids. These results are in agreement with the data published by Pappu *et al.* (2006) and Hafez *et al.* (2013; 2014). Comparative sequence homology with phylogenetic analyses revealed that our isolate shared maximum sequence identity with another Egyptian IYSV isolate (Acc# JN541273) at the nucleotide level (99%) and the amino acid (99%) levels.

Generally, plant virus analyses include ORF(s) identification, sequence alignment, homology searching, gene prediction and motif recognition (Yan 2008). Moreover, the predictions of features such as phosphorylation and glycosylation sites are necessary for the analysis of the structure–function relationships of proteins encoded in plant virus genomes (Yan 2008). A computational examination of the N protein indicated that four types of motifs with 20 different sites were detected. Motives like these are involved, and play different roles, in the virus activity, in addition to its regulation and stability. Fascinatingly, most of the detected and identified motifs are related to phosphorylation-related sites and are similar to those obtained in our previous study (Hafez *et al.* 2014). It is well known that the phosphorylation of viral and cellular proteins has major impacts on viral infection, replication, and cytotoxicity in a host cell (Keating and Striker 2012). Consequently, Jakubiec and Jupin (2007) reported that viral protein's stability, activity, and interactions with other cellular and viral proteins could be regulated by the addition of a phosphate group. Six sites with N-myristoylation motif were also detected on the IYSV-N protein; these N-myristoylation motifs are critical during the viral infection process. Fondong *et al.* (2007) reported that the presence of N-myristoylation motif on AC4 protein is

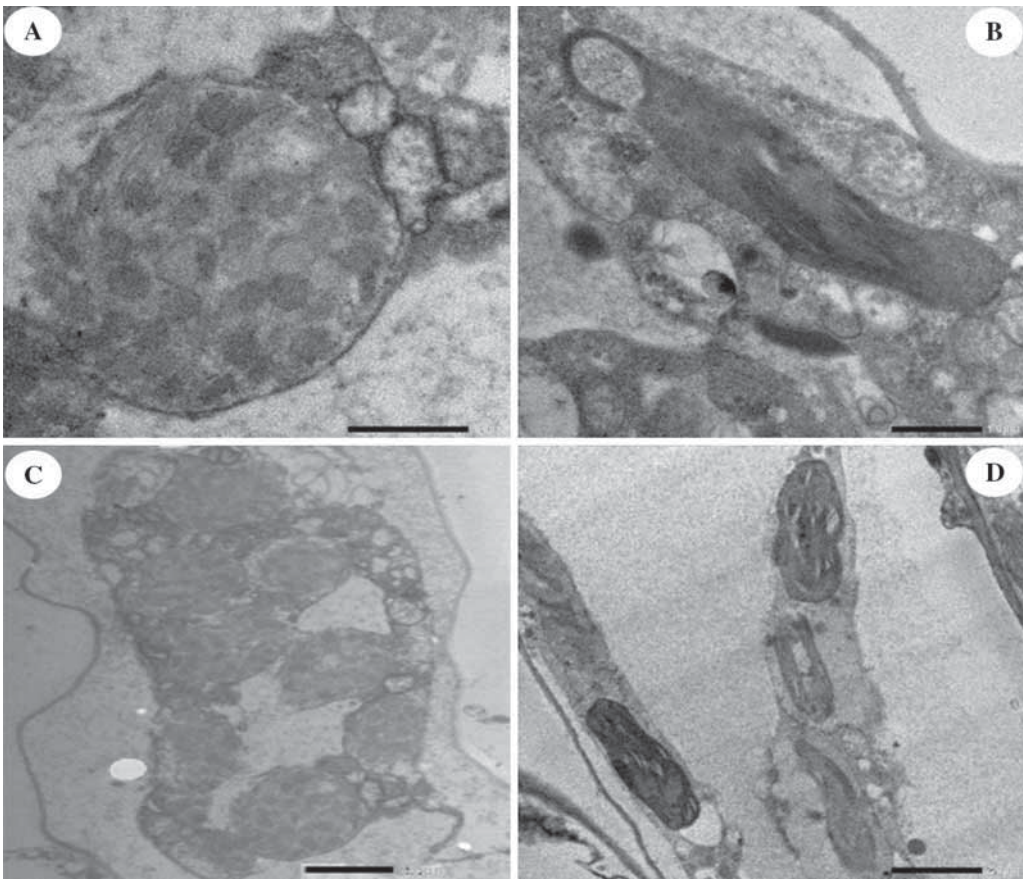

Figure 7. Electron micrographs of ultrathin sections showing cytopathological effects of IYSV on onion tissues chloroplasts at 20 dpi. (**A**) Chloroplast with irregular out-membrane structures and broken envelope with the presence of numerous spherical particles inside it, (**B**) chloroplast with long stromule, (**C**) accumulation of IYSV-like particles in chloroplast with more chloroplast aggregation, (**D**) partially destroyed and deformed chloroplasts with disorganised grana and stroma lamella. Scale Bars: A) 1 μm, X = 8000, B) 1 μm, X = 6000. C) 2 μm, X = 2000, D) 2 μm, X = 3000. Arrows indicate the cytoparhology defection.

responsible for plasma membrane targeting and pathogenicity of thr *East African cassava mosaic Zanzibar virus*.

Many previous studies indicated that chloroplast structure and components changes are often associated with viral infection (Li *et al.* 2016). Moreover, recent reports revealed that viral chlorosis-related symptoms were correlated with the changes in chloroplast structure and membrane complexes (Bhattacharyya *et al.* 2017; Zhao *et al.* 2019). During the hypersensitive reaction of N-mediated TMV resistance, swelled chloroplasts and membrane burst were observed before tonoplast ruptured (da Graça and Martin 1975). Our results showed that the chloroplasts in the IYSV-infected onion plants suffered from dramatic malformations. Briefly, a broken envelope of swollen chloroplasts with thinner and irregular outer membrane structures was detected. Additionally, aggregated chloroplasts, disorganised grana and stroma lamella were clearly observed. A presence of spherical IYSV-like particles accumulated in the chloroplast, which are closely similar to inclusion bodies, were also detected. This observation agrees with Zhao *et al.* (2019) who reported that the ultrastructure of *Rice stripe virus* (RSV) infected *N. benthamiana* plants showed many chloroplasts malformations like swollen or globular chloroplasts in addition to a reduction or irregular arrangement of stroma lamella. Clearly, the stromules facilitate the magnification and transport of defensive signals into the nucleus (Zhao *et al.* 2016). Many studies reported that CMV and PVX diseases are associated with chloroplast ultrastructure changes such as structural alteration of chloroplast membranes and grana stacks (Qiao *et al.* 2009; Mazidah *et al.* 2012). Moreover, *Abutilon mosaic virus* (AbMV) replicates the inside the chloroplast and induces the biogenesis of the stromule network (Groning *et al.* 1990). We assume that the TEM results indicate that the chloroplast ultrastructural changes could be a part of the defence response and the state of malformation could be an indicator of the virus incidence and severity. Moreover, the chloroplasts structure became clearly abnormal in onion leaves infected with IYSV after 20 dpi when compared with earlier observations. This finding and assumption confirm the results obtained by da Graça and Martin (1975) who postulated that the chloroplast malformation indicates a defence response in compatible host–virus interaction.

The repression of expression of chloroplast-related genes indicated that there are irreplaceable interactions between the virus and the chloroplasts ending in the appearance of viral symptoms (Das *et al.* 2019). Babu *et al.* (2008) reported that the expression levels of 52 chloroplast-related genes were up-regulated at 17 dpi of infected *Arabidopsis thaliana* - plants with *Plum pox virus* (PPV). Induction of these genes mainly targeted the maintenance of the plant cell morphology and functions (Babu *et al.* 2008). On the other hand, Cho *et al.* (2015) suggested that RSV affects the transcriptome of the chloroplasts, rather than that of mitochondria, directly or indirectly, and that it could occur either in the early or late stages of infection by RSV suppressing and down-regulating many of chloroplast-related genes.

It was observed that the differentially expressed genes were highly observed at 5, 10 and 15 dpi, but the highest expression level reached its peak at 15 dpi. As the bands' intensity is a good indicator reflecting viral effects on the plant transcriptome, the higher up-regulated band with 450 bp at 15 dpi was purified and sequenced. The nucleotide sequence analysis revealed that this gene encodes a chloroplast-related protein (Acc# MH746819). Based on the annotated sequence, specific degenerated primers amplifying 158 bp within the chloroplast-related gene were designed and used for qRT-PCR. Besides the high validity of the designed primer in qRT-PCR, the DD-PCR results confirmed that the highest expression level of the chloroplast-related gene reached its peak after 15 dpi. The two molecular tools – DD-PCR and qRT-PCR – confirmed the biological appearance of the viral symptoms on the plant leaves, the symptoms starting its appearance from day 13 and completing their standard performance on day 15. This assumption was confirmed by the results of Satoh *et al.* (2011) who postulated that *Rice dwarf virus* affects the plant gene responses, which regulated differently. In addition, the authors observed that symptom severity was correlated with defence-related genes, and the genes regulated the plant cell development processes. Our results are in agreement with this, indicating a presence of fluctuation in the expression of the chloroplast-related gene. This agrees with Bhattacharyya and Chakraborty (2018) who postulated that the chloroplast is often originally targeted by viruses and it plays an important role in plant defence against pathogen attack. Due to the deficiency in gene silencing mechanism in the chloroplast, chloroplasts compensate by triggering an immune response from other plant cell organelles to resist the viral propagation (Caplan *et al.* 2015).

It is well known that the mitochondrion is an important organelle in cells for energy supply and that mitochondrial dysfunction is mostly associated with plant diseases. Cytoplasmic male sterility is a mysterious natural phenomenon controlled and resulting in an interaction between nuclear and mitochondrial DNAs (Hu *et al.* 2014). Moreover, male sterility could be induced through spontaneous mutations either in nuclear or cytoplasmic genes (Schnable and Wise 1998). Different studies on chloroplast deficiency in male sterility have been performed through natural and artificial mutations in chloroplast genes, concluding that chloroplast deficiency mostly resulted in cytoplasmic male sterility (Akagi *et al.* 2004; Liu *et al.* 2004).

A phylogenetic tree data analysis is essential in molecular studies where it represents the evolutionary relationships between organisms and genomic sequences. In this study, the phylogenetic tree and multiple sequences alignment data revealed that the chloroplast-related gene (Acc# MH746819) showed 99% similarity with *Allium cepa* genotype normal (N) male fertile chloroplast (Acc# KF728079). Edwardson and Corbett (1961) postulated that flowers fertility, partial sterility, and male sterility in the same plant could be caused by infection of plants viruses; this could have occurred either in symptomless, mild and/or severe symptoms in the same plant. They confirmed the presence of identity between the factors controlling cytoplasmic sterility in petunias and viruses infecting this plant. Atanasoff (1971) reported that viral transmission might cause on cytoplasmic male sterility and assumed that the cytoplasmic factors are mainly viruses in most infected plants. Brewbakers (1964) who speculated that the cytoplasmic factors are viruses or virus-like factors reported the same observation. Similarly, viruses make a reduction and sometimes clearance of the chlorophyll in the infected plant tissues (Plattt *et al.* 1979).

5. Conclusions

Besides the isolation and molecular characterisation of a new Egyptian IYSV isolate, both biological and molecular studies under this investigation confirmed the interactions between the viral proteins and chloroplasts resulting in the interruption of chloroplast structures and functions. Moreover, a degenerate primer set amplifying a fragment of 158 bp within the chloroplast-related gene of onion tissues may be useful to study the expression levels of this gene in onion plants under stress conditions. Both virus infection and mutation in chloroplasts and/or in mitochondria could result in male sterility in the infected plants. This interaction between the viral particles and the genes that control either mitochondrial DNA and/or chloroplasts synthesis process, affect the plant defence and help the virus gain more chances for propagation, movement, and distribution in the infected plant tissues. This assumption reflects the fluctuation of expression of the chloroplast-related gene under this investigation. It could be considered as one of the genes controlled by the IYSV. In addition, the up- and down-regulation of this gene may be associated with the viral propagation.

References

Abdelkhalek A, ElMorsi A, AlShehaby O, Sanan-Mishra N and Hafez E 2018 Identification of genes differentially expressed in *Iris yellow spot virus* infected onion. *Phytopathol. Mediterr.* **57** 334–340

Akagi H, Nakamura A, Yokozeki-Misono Y, Inagaki A, Takahashi H, Mori K and Fujimura T 2004 Positional cloning of the rice Rf-1 gene, a restorer of BT-type cytoplasmic male sterility that encodes a mitochondria targeting PPR protein. *Theor. Appl. Genet.* **108** 1449–1457

Atanasoff D 1971 The viral nature of cytoplasmic male sterility in plants. *Phytopath. Z.* **70** 306–322

Babu M, Griffiths JS, Huang TS and Wang A 2008 Altered gene expression changes in Arabidopsis leaf tissues and protoplasts in response to *Plum pox virus* infection. *BMC Genomics* **9** 325

Bhattacharyya D and Chakraborty S 2018 Chloroplast: the Trojan horse in plant-virus interaction. *Mol. Plant Pathol.* **19** 504–518

Brewbaker JL 1964 *Agricultural Genetics*, Prentice-Hall, Inc, Englewood Cliffs, Jersey, USA, pp 42–45

Caplan JL, Kumar AS, Park E, Padmanabhan MS, Hoban K, Modla S, Czymmek K and Dinesh-Kumar SP 2015 Chloroplast stromules function during innate immunity. *Dev. Cell* **34** 45–57

Caplan JL, Mamillapalli P, Burch-Smith TM, Czymmek K and Dinesh-Kumar SP 2008 Chloroplastic protein NRIP1 mediates innate immune receptor recognition of a viral effector. *Cell* **132** 449–462

Cho WK, Lian S, Kim SM, Seo BY, Jung JK and Kim KH 2015 Time-course RNA-seq analysis reveals transcriptional changes in rice plants triggered by *Rice stripe virus* infection. *PloS One* **10** e0136736

Clark MF and Adams AN 1977 Characteristics of the microplate method of enzyme-linked immunosorbent assay for the detection of plant viruses. *J. Gen Virol*. **34** 475–483

da Graça JV and Martin MM 1975 Ultrastructural changes in *tobacco mosaic virus*-induced local lesions in *Nicotiana tabacum* L cv "Samsun NN". *Physiol. Plant Pathol*. **7** 287–291

Das PP, Lin Q and Wong SM 2019 Comparative proteomics of *Tobacco mosaic virus*-infected *Nicotiana tabacum* plants identified major host proteins involved in photosystems and plant defence. *J. Proteom.* **194** 191–199

de Torres Zabala M, Littlejohn G, Jayaraman S, Studholme D, Bailey T, Lawson T, Tillich M, Licht D, Bölter B, Delfino L, Truman W, Mansfield J, Smirnoff N and Grant M 2015 Chloroplasts play a central role in plant defence and are targeted by pathogen effectors. *Nat. Plants* **1** 15074

Edwardson JR, Christie RG, Purcifull DE and Petersen MA 1993 Inclusions in diagnosing plant virus diseases; in *Diagnosis of plant virus diseases* (ed) RE Matthews (CRC Press, Boca Raton, Florida, USA) pp 101–128

Edwardson JR and Corbett MK 1961 Asexual transmission of cytoplasmic male sterility. *Genetics* **47** 390–396

ElMorsi A, Abdelkhalek A, AlShehaby O and Hafez E 2015 Pathogenesis-related genes as tools for discovering the response of onion defence system against *Iris yellow spot virus* infection. *Botany* **93** 735–744

FAO (Food and Agricultural Organization of the United Nations), 2017 statistics. *http://faostatfao.org*

Fauquet CM, Mayo MA, Maniloff J, Desselberger U and Ball LA 2005 Virus taxonomy *Eighth Report of the International Committee on Taxonomy of Viruses*, Elsevier Academic Press, San Diego, California

Fondong VN, Reddy RV, Lu C, Hankoua B, Felton C, Czymmek K and Achenjang F 2007 The consensus N-myristoylation motif of a geminivirus AC4 protein is required for membrane binding and pathogenicity. *Mol. Plant Microbe Interact*. **20** 380–391

Gent DH, du Toit LJ, Fichtner SF, Krishna Mohan S, Pappu HR and Schwartz HF 2006 *Iris yellow spot virus*: an emerging threat to onion bulb and seed production. *Plant Dis.* **90** 1468–1480

Groning BR, Frischmuth T and Jeske H 1990 Replicative form DNA of *Abutilon mosaic virus* is present in plastids. *Mol. Gen. Genet*. **220** 485–488

Hafez E, El-Morsi AA and Abdelkhalek AA 2011 Biological and molecular characterisation of the fig mosaic disease. *Mol. Pathogens* **2** 10–14

Hafez EE, Abdelkhalek AA, Abeer SA and Galal FH 2013 Altered gene expression: induction/suppression in leek elicited by *Iris yellow spot virus* infection (IYSV) Egyptian isolate. *Biotechnol. Biotechnol. Equip*. **27** 4061–4068

Hafez EE, Abdelkhalek AA, El-Morsi AA and El-Sbahaby OA 2012 First report of *Iris yellow spot virus* infection of garlic and Egyptian leek in Egypt. *Plant Dis*. **96** 594

Hafez EE, El-Morsi AA, El-Shahaby OA and Abdelkhalek AA 2014 Occurrence of *Iris yellow spot virus* from onion crops in Egypt. *Virus Disease* **25** 455–459

Hu J, Huang W, Huang Q, Qin X, Yu C, Wang L, Li S, Zhu R and Zhu Y 2014 Mitochondria and cytoplasmic male sterility in plants. *Mitochondrion J.* **19** 282–288

Jakubiec A and Jupin I 2007 Regulation of positive-strand RNA virus replication: the emerging role of phosphorylation. *Virus Res.* **129** 73–79

Karimi FL, Mardi M and Ebrahimi MA 2013 Quantitative expression analysis of candidate genes for *Septoria tritici* blotch resistance in wheat (*Triticum aestivum* L). *Prog. Biol. Sci.* **3** 72–78

Keating JA and Striker R 2012 Phosphorylation events during viral infections provide potential therapeutic targets. *Rev. Med. Virol.* **22** 166–181

Li S, Li X, Sun L and Zhou YJ 2012 Analysis of *rice stripe virus* whole-gene expression in rice and in the small brown plant hopper by real-time quantitative PCR. *Acta Virol.* **56** 75–79

Li Y, Cui H, Cui X and Wang A 2016 The altered photosynthetic machinery during compatible virus infection. *Curr. Opin. Virol.* **17** 19–24

Liang P and Pardee A 1992 Differential Display of eukaryotic messenger RNA by means of the polymerase chain reaction. *Science* **257** 967–971

Liu XQ, Xu X, Tan YP, Li SQ, Hu J, Huang JY, Yang DC, Li YS and Zhu YG 2004 Inheritance and molecular mapping of two fertility-restoring loci for Honglian gametophytic cytoplasmic male sterility in rice (*Oryza sativa* L). *Mol. Genet. Genomics* **271** 586–594

Livak KJ and Schmittgen TD 2001 Analysis of relative gene expression data using real-time quantitative PCR and the 2(-Delta Delta C(T)) method. *Methods* **25** 402–408

Martelli GP and Russo M 1984 Use of thin sectioning for the visualization and identification of plant viruses. *Methods Virol.* **8** 143–224.

Mazidah M, Lau WH, Yusoff K, Habibuddin H and Tan YH 2012 Ultrastructural features of *Catharanthus roseus* leaves infected with *cucumber mosaic virus* Pertanika. *J. Trop. Agric. Sci.* **35** 85–92

Murai T and Loomans AJM 2001 Evaluation of an improved method for mass-rearing of thrips and a thrips parasitoid. *Entomol. Exp. Appl*. **101** 281–289

Otulak K, Koziel E and Garbaczewska G 2014 "Seeing is believing" The use of light, fluorescent and transmission

electron microscopy in the observation of pathological changes during different plant-virus interactions; in *Microscopy: Advances in Scientific Research and Education* (ed) A Mendez-Vilas, 6th ed, (Formatex Research Center, Badajoz, Spain) **1** 367–376

Pappu HR, duToit LJ, Schwartz HF and Mohan SK 2006 Sequence diversity of the nucleoprotein gene of *iris yellow spot virus* (Genus *Tospovirus*, Family *Bunyaviridae*) isolates from the western region of the United States. *Arch. Virol*. **151** 1015–1025

Platt SG, Henriques F and Rand L 1979 Effects of virus infection on the chlorophyll content, photosynthetic rate and carbon metabolism of *Tolmiea menziesii*. *Physiol. Plant Pathol*. **15** 351–365

Qiao Y, Li HF, Wong SM and Fan ZF 2009 Plastocyanin transit peptide interacts with *Potato virus X* coat protein, while silencing of plastocyanin reduces coat protein accumulation in chloroplasts and symptom severity in host plants. *Mol. Plant Microbe Interact.* **22** 1523–1534

Satoh K, Shimizu T, Kondoh H, Hiraguri A, Sasaya T, Choi IR, Omura T and Kikuchi S 2011 Relationship between symptoms and gene expression induced by the infection of three strains of *Rice dwarf virus*. *PLoS One.* **6** e18094

Schnable P and Wise RP 1998 The molecular basis of cytoplasmic male sterility and fertility restoration. *Trends in Plant Sci.* **3** 175–180

Seo EY, Nam J, Kim HS, Park YH, Hong SM, Lakshman D, Bae H, Hammond J and Lim HS 2014 Selective interaction between chloroplast β-ATPase and TGB1L88 retards severe symptoms caused by *Alternanthera mosaic virus* infection. *Plant Pathol. J.* **30** 58–67

Serrano I, Audran C and Rivas S 2016 Chloroplasts at work during plant innate immunity. *J. Exp Bot.* **67** 3845–3854

Vajire D, Thakare K, Soluke R and Aparna T 2017 The possibilities of the prediction of heterosis in elite lines of onion based on the assessment of genetic diversity. *EC Microbiology* **10** 211–219

Whitham SA, Yang C and Goodin MM 2006 Global impact: elucidating plant responses to viral infection. *Mol. Plant Microbe Interact*. **19** 1207–1215

Yan Q 2008 Bioinformatics databases and tools in virology research: an overview. *In Silico Biol.* **8** 71–85

Zhao J, Xu J, Chen B, Cui W, Zhou Z, Song X, Chen Z, Zheng H, Lin L, Peng J, Lu Y, Deng Z, Chen J and Yan F 2019 Characterization of proteins involved in chloroplast targeting disturbed by *Rice Stripe Virus* by novel protoplast-chloroplast proteomics. *Int. J. Mol Sci.* **20** 253

Zhao J, Zhang X, Hong Y and Liu Y 2016 Chloroplast in plant-virus interaction. *Front Microbiol*. **7** 1565

Corresponding editor: Manchikatla Venkat Rajam